The PAMELA experiment in space

V. Bonvicini[a,*], G. Barbiellini[a], M. Boezio[a], E. Mocchiutti[a], P. Schiavon[a],
G. Scian[a], A. Vacchi[a], G. Zampa[a], N. Zampa[a], D. Bergström[b], P. Carlson[b],
T. Francke[b], J. Lund[b], M. Pearce[b], M. Hof[c], W. Menn[c], M. Simon[c], S.A.
Stephens[d], M. Ambriola[e], R. Bellotti[e], F. Cafagna[e], F. Ciacio[e], M. Circella[e],
C. De Marzo[e], N. Giglietto[e], B. Marangelli[e], N. Mirizzi[e], P. Spinelli[e], O. Adriani[f],
M. Boscherini[f], R. D'Alessandro[f], N. Finetti[f], M. Grandi[f], P. Papini[f], A. Perego[f],
S. Piccardi[f], P. Spillantini[f], E. Vannuccini[f], S. Bartalucci[g], L. Marino[g], M. Ricci[g],
B. Spataro[g], V. Bidoli[h], M. Casolino[h], M.P. De Pascale[h], G. Furano[h],
A. Morselli[h], P. Picozza[h], R. Sparvoli[h], L.M. Barbier[i], E.R. Christian[i],
J.F. Krizmanic[i], J.W. Mitchell[i], J.F. Ormes[i], R.E. Streitmatter[i], U. Bravar[j],
S.J. Stochaj[j], S. Bertazzoni[k], A. Salsano[k], G. Bazilevskaja[l], A. Grigorjeva[l],
R. Mukhametshin[l], Y. Stozhokov[l], E. Bogomolv[m], S. Krutkov[m], G. Vasiljev[m],
A.M. Galper[n], S.V. Koldashov[n], M.G. Korotkov[n], V.V. Mikhailov[n],
A.A. Moissev[n], J.V. Ozerov[n], S.A. Voronov[n], Y. Yurkin[n], G. Castellini[o],
A. Gabbanini[o], F. Taccetti[o], M. Tesi[o], V. Vignoli[o]

[a] INFN section and Physics Department, University of Trieste, Via A. Valerio 2, 34127 Trieste, Italy
[b] Royal Institute of Technology (KTH), Stockholm, Sweden
[c] Universität Siegen, Siegen, Germany
[d] Tata Institute of Fundamental Research, Bombay, India
[e] INFN section and Physics Department, University of Bari, Bari, Italy
[f] INFN section and Physics Department, University of Firenze, Firenze, Italy
[g] Laboratori Nazionali INFN, Frascati, Italy
[h] INFN section and Physics Department, University of Tor Vergata, Roma, Italy
[i] NASA/Goddard Space Flight Center, Greenbelt, USA
[j] New Mexico State University, Las Cruces, USA
[k] Electronic Engineering Department, University of Tor Vergata, Roma, Italy
[l] Lebedev Physical Institute, Russia
[m] Ioffe Physical Technical Institute, Russia
[n] Moscow Engineering and Physics Institute, Moscow, Russia
[o] Istituto di Ricerca Onde Elettromagnetiche CNR, Firenze, Italy

*Corresponding author. Tel.: + 39-40-3756224; fax: + 39-40-3756258.
E-mail address: bonvicini@trieste.infn.it (V. Bonvicini).

Abstract

We provide in this paper a status report of the space experiment PAMELA. PAMELA aims primarily to measure the flux of antiparticles, namely antiprotons and positrons, in cosmic rays with unprecedented statistics over a large energy range. In addition, it will measure the light nuclear components of cosmic rays, investigate phenomena connected to Solar and Earth physics and it will search for cosmic ray antinuclei with sensitivity better than 10^{-7} in the $\overline{\text{He}}$/He ratio. PAMELA consists of a magnet spectrometer, a transition radiation detector, an imaging calorimeter, a time of flight system and an anticoincidence detector. The apparatus will be installed on board of the Russian satellite of the Resurs type in a polar orbit at about 680 km of altitude. The launch is foreseen for late 2002/early 2003. © 2001 Elsevier Science B.V. All rights reserved.

1. The PAMELA experiment

The PAMELA experiment is the main part of the Russian Italian Mission (RIM) program, which foresees several space missions with different scientific programs. The first of these missions (RIM-1 experiment) studied the isotopic composition of cosmic-ray nuclei and of solar energetic particles by means of the silicon telescope NINA [1], carried by the Russian polar orbit satellite Resurs-04. The NINA instrument was launched succesfully from Bajkonur on July 10th, 1998 and has collected a significant amount of data [2].

The PAMELA experiment (RIM-2 mission) has the scientific goal of measuring the cosmic radiation over a wide energy range. The apparatus will be installed on board of the Russian Resurs satellite and will be launched in late 2002/early 2003. Its sun-synchronous, 680 km polar orbit will allow the low-energy cosmic rays to be measured while the instrument is near the poles.

The main observational objectives of the PAMELA experiment can be summarized as follows:

- measurement of the $\bar{p}$ flux from 80 MeV to 190 GeV;
- measurement of the e^+ flux from 50 MeV to 270 GeV;
- search of antinuclei with a sensitivity of $\sim 10^{-7}$ in the $\overline{\text{He}}$/He ratio;
- measurement of the nuclear component flux (from H to C) from 100 MeV/n to 200 GeV/n;
- measurement of the e^- flux from 50 MeV to 400 GeV.

Additional objectives are the following:

- monitoring of the cosmic rays solar modulation during and after the 23rd maximum of the solar activity;
- study of the time and energy distributions of the energetic particles emitted in solar flares and coronal mass ejections;
- study of the anomalous component of cosmic rays;
- study of stationary and disturbed fluxes of high-energy particles in the Earth magnetosphere.

PAMELA will therefore continue and extend the measurements so far performed by the WiZard Collaboration by means of balloon-borne detectors [3].

2. The PAMELA apparatus

PAMELA uses a detector layout similar to the one used by the WiZard Collaboration in its balloon experiments [3]. The apparatus is composed of the following subdetectors, arranged as in Fig. 1.

- a magnetic spectrometer (SPE), capable of determining the sign and the absolute value of the electric charge with a very high confidence
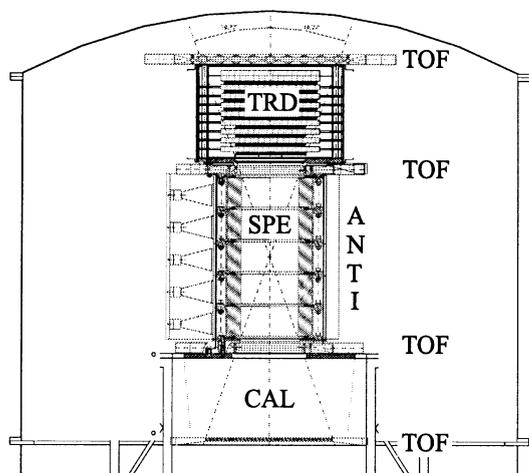
Fig. 1. The PAMELA telescope.

level and measuring the momentum of the particles up to the highest energies;

- a plastic scintillator system, which includes a time-of-flight counter (TOF) and an anti-coincidence system (ANTI) which identifies those particles entering the spectrometer from outside its geometrical acceptance;
- an electromagnetic imaging calorimeter (CAL), which measures the energy released by the interacting e^- and e^+ and reconstructs the spatial development of the shower, allowing to distinguish electromagnetic showers from hadronic showers and from non-interacting particles;
- a Transition Radiation Detector (TRD), which gives a threshold velocity measurement, complementing the calorimeter in the particle identification.

The total height of the apparatus is 113.5 cm and the lateral dimensions of the detectors have been determined in such a way to fully cover the acceptance of the magnet spectrometer.

The design of the apparatus has been performed taking into account the strict mass and power consumption limitations imposed by the satellite environment and the mechanical stability required to withstand the stresses during the launch phase. Prototypes of each subdetector have been built and tested for vibration and shock resistance. The performances of each detector have been exten-

sively studied at particle beam tests. In the following, we describe the characteristics and performances of the main components of the PAMELA apparatus.

3. The magnet spectrometer

The magnetic spectrometer of the PAMELA experiment consists of 5 modules of permanent magnets, made of a sintered Nd–B–Fe alloy, interleaved by 6 silicon detector planes. The available cavity is 445 mm tall with a section of $131 \times 161 \, \text{mm}^2$, giving a geometrical factor of $20.5 \, \text{cm}^2\text{sr}$. The mean magnetic field inside the cavity is $\sim 0.4 \, \text{T}$, resulting in a Maximum Detectable Rigidity of $740 \, \text{GV}/c$ if a spatial resolution of $4 \, \mu\text{m}$ along the bending view is assumed. The spectrometer simulation shows that, with such performances, the p and e^- spillover sets the upper energy limits in the $\bar{\text{p}}$ and e^+ flux measurements given in Section 1.

Each detector plane of the tracking system is composed of three ladders obtained by gluing together two microstrip silicon sensors and an aluminium oxide hybrid that contains the front-end electronics (Fig. 2).
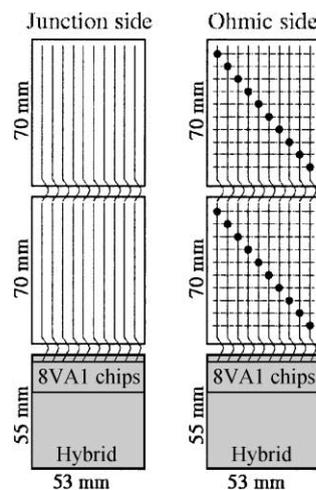

Fig. 2. Schematic view of both sides of a ladder. The vertical lines are the readout strips. The horizontal dashed lines are the n^+-type implanted strips on ohmic side. Dots represent the ohmic contacts between the two metal layers.

The ladders are realized using double sided, double metal, AC-coupled silicon sensors produced by Hamamatsu Photonics. Both sides of the sensor are segmented, in such a way that the measurement of two independent coordinates is possible. A second metal layer is present on the ohmic side in order to make all the readout lines parallel, so that both sides can be read from the same edge. Decoupling capacitors are directly integrated on the sensors, simplifying the mechanical structure. This kind of sensors thus allows extremely compact detectors to be realized.

The low noise, low power, VLSI VA1 chip has been selected for the front-end section. The use of low-noise front-end electronics is of great importance since the spatial resolution of the detector is strongly related to its signal-to-noise ratio.

Prototypes of the silicon sensors have been extensively calibrated with particle beams during the past few years. These tests have been performed using minimum and non-minimum ionizing particles in order to study the performances of the detector to significantly different energy releases [4,5]. For purposes of illustration, we show in Fig. 3, the distribution of positional residuals for the junction side obtained with a telescope of three ladders for π^- of $3.5\,\text{GeV}/c$ which impinged perpendiculary on the sensors. The applied position finding algorithm is the η-

algorithm [6], that gives a spatial resolution of $2.9 \pm 0.1\,\mu\text{m}$. The junction side shows a larger signal-to-noise ratio ($S/N \sim 49$) and a better spatial resolution. For this reason, it will be used to measure the position along the bending view.

4. The calorimeter

The calorimeter has been designed in such a way to: (i) extract the antiproton signal from the large background generated by the electron flux, with an efficiency of more than 90% and a rejection power of 10^{-4}; (ii) identify positrons in the background generated by protons, with an efficiency of more than 90% and a rejection power better than 10^{-4}.

The detector is a sampling calorimeter made of silicon sensor planes interleaved with plates of tungsten absorber. The instrument is characterised by its high granularity, both in the longitudinal (Z) and in the transversal (X and Y) directions. In the Z direction, the granularity is determined by the thickness of layers of the absorbing material. Each tungsten layer has a thickness of $0.26\,\text{cm}$, which corresponds to $0.74X_0$ (radiation lengths). Since there are 22 tungsten layers, the total depth is $16.3X_0$ (i.e. 0.6 interaction lengths).

The transverse granularity is given by the segmentation of the silicon detectors into large strips, as explained below. Each tungsten plane is sandwiched between two layers of silicon detectors, i.e. the layout of single detection plane is Si-X/W/Si-Y. For each view (X or Y) there are nine silicon detectors, arranged in a square matrix of 3×3 detectors. Since each silicon detector has a surface of $8 \times 8\,\text{cm}^2$, the total sensitive area is $24 \times 24\,\text{cm}^2$. The total volume is $24 \times 24 \times 18\,\text{cm}^3$. Each detector has 32 strips and each strip is connected to those belonging to the two detectors of the same row (or column), so that the number of electronics channels per plane is $32 \times 3 \times 2 = 192$ and the total number of channels is $192 \times 22 = 4224$.

The mechanical structure is based on a modular concept. Two detection planes form a ''detection module''. In a module, the two detection planes are kept together by a frame to which they are
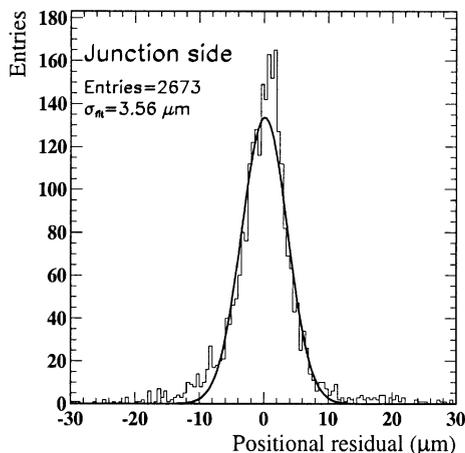

Fig. 3. Positional residual distribution for π^- of $3.5\,\text{GeV}/c$, from a beam test performed at the PS facility at CERN.
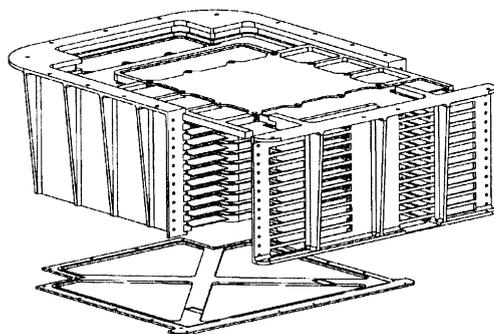
Fig. 4. Assembly view of the whole calorimeter structure.

$$y = 4.8593 + 5.1099 \times R*2 = 1.000$$

Fig. 5. CR1.4P linear range.

bolted at the edge of the absorber plate. All modules are independent and fully extractable: they are inserted like "drawers" into the main mechanical structure and then locked by a cover, as shown in Fig. 4. The read-out boards are also located in this structure on two "dummy plates". The total calorimeter mass (including electronics and cables) is 110 kg.

The front-end electronics is based on a VLSI ASIC specifically designed for the PAMELA calorimeter: the CR1.4P chip [7]. The main design characteristics of this chip are the wide dynamic range (1400 minimum ionising particles, 1 MIP $\simeq$ 5.1 fC for 380 μm thick silicon detectors), the ability to cope with a very large (up to $\simeq$ 180 pF) detector capacitance, the good noise performance ($\simeq 2700\,e^-$ rms $+ 5\,e^-$/pF and the low power consumption (<100 mW/chip). Each circuit has 16 channels and each channel comprises a charge sensitive preamplifier, a shaping amplifier, a track-and-hold circuit and an output multiplexer. A self-trigger system and an input calibration circuit are also integrated in the chip. Fig. 5 shows the measured linear range in one channel of the chip. Over the full range, the maximum deviation from the fit line is $<2.5\%$ and the average linearity is better than 1%.

In addition to housing the silicon detectors and the front-end chips, the front end boards also house the data conversion electronics. On each front-end board, the six CR1.4P outputs are connected to a 16-bit ADC (with serial digital output) through an analogue multiplexer and an
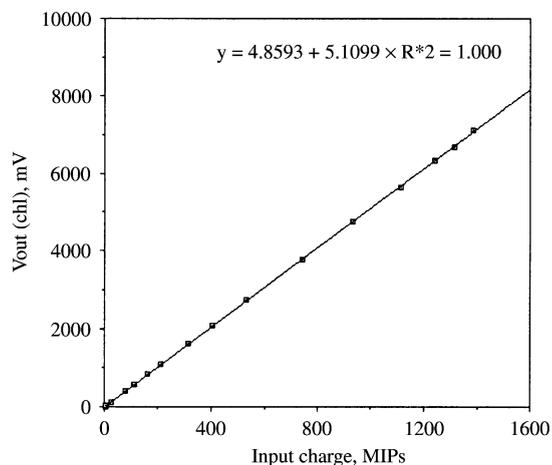
operational amplifier. Fig. 7 shows a complete front-end board mounted in a module.

The silicon detectors for the PAMELA calorimeter are large area devices ($8 \times 8\,cm^2$ each), 380 μm thick and segmented into 32 large strips with a pitch of 2.4 mm. They are fabricated on high-purity, high-resistivity ($\geq 7\,k\Omega$ cm), n-type silicon substrate. In order to avoid the use of a conductive epoxy glue for gluing the detectors onto the printed circuit boards and for protecting the devices from the large mechanical stress that these type of glues can induce during polymerization, the bias voltage is brought directly on the junction side of the devices via wire bonding.

The interconnection technique for the assembly of the detection planes is organized into three steps: as a first step, the printed circuit boards are fixed to the corresponding tungsten plates. Three detectors are glued on a specially designed 75 μm thick kapton layer with a siliconic glue. Then, the wire bonding of the corresponding strips on each detector is performed; this forms a "ladder". Finally, three ladders are glued onto the supporting printed circuit board, again by using a special siliconic glue, to form 3×3 silicon detector matrix of one view.

The performance of the calorimeter has been extensively investigated with simulations developed from the experimental results of the previous
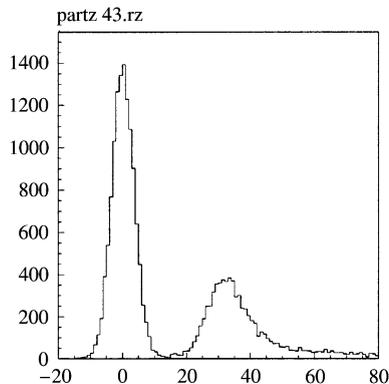
partz 43.rz

Fig. 6. Signal distribution on one strip from minimum ionizing particles.

Fig. 7. Artistic view of a 32 straw tube module.

balloon-flight calorimeter. Furthermore, a partially equipped version of the calorimeter underwent a series of test-beams in May 2000 (CERN PS) and July/August 2000 (CERN SPS). The instrument was equipped with six X-type views. Fig. 6 shows the signal distribution on one strip from minimum ionizing particles (SPS data). As can be seen, the signal is well separated from the pedestal and the most probable value of the distribution corresponds to a signal-to-noise ratio of 9:1, thus confirming the expected performance.

5. The TRD

The TRD will perform particle identification by detecting the transition radiation released by ultrarelativistic charged particles. It is expected to provide a hadron rejection factor of the order of a few percent at a high detection efficiency for electrons.

The detector, located at the top of the detector stack, has a modular design. It is composed of 9 sensitive planes each preceded by a radiator layer in which the emission of transition radiation eventually takes place.

The basic component is a straw tube of 4 mm diameter and 28 cm length, made of 30 μm thin Kapton foil copper-coated on the inner side. Inside the tube a tungsten anode wire, 25μm diameter, is stretched to a tension of ~ 70 g. The tubes are
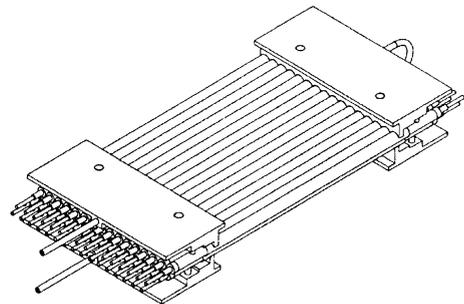
arranged in two layers of 16. These layers are glued in a close pack configuration, in order to get a uniform X-ray yield. An artistic view of this 32 straw module is shown in Fig. 7.

The straw tubes are filled with an 80:20 mixture of Xe and CO_2 and work at an operating voltage of 1400 V. Tests show that this is the optimal configuration in order to maximize the photon detection efficiency and operate the tubes in a moderate gain region. The modules are housed on a special frame to form detection planes. The TRD is made of 5 of planes of 4 modules placed above 4 planes of 3 modules for a total of 32 modules, i.e. 1024 straw tubes.

The WiZard collaboration already launched a TRD in the TS93 balloon-borne detector [8,9]. Based on this experience and Monte-Carlo simulations a carbon fiber radiator with density of 60 g/l has been chosen for this detector.

A critical point in the mechanical design is the presence of a gas feeding system and the high-voltage distribution in a small volume. In order to solve this problem the 16 straw tubes forming half of a 32 straw module are kept in place by means of brass plates that also act as manifolds for the gas mixture. Besides, "T"-shaped pipes are glued to the straw ends and inserted in the brass plate to provide: gas circulation inside the single tubes, housing for the electrical connector, ground connection. The high voltage connection is provided by plug-ins soldered to the anode wire and placed, inside a fiber glass insulting pipe, in the "T" shape piece.

Straw tube modules have been tested for resistance to vibrations as well as to overpressure,

showing no modification in the electrical and mechanical characteristics. Prototypes have also been tested for gas leaks showing a rate of 3–4×10^{-3} (Torr 1)/s at 1 atm overpressure, for Argon-based mixtures.

A charge integration technique has been chosen for data acquisition of the TRD, based on results from particle beam tests. These tests show that a pion rejection factor of the order of 5% at an electron efficiency of $\sim 90\%$ is feasible. The front-end electronics will be based on the CR1.4P VLSI chip described in the previous section.

6. Conclusions

PAMELA is a powerful instrument that will give results of great scientific relevance in several fields of cosmic ray research. Prototypes of the main detectors have been built and tested thoroughly. All these tests have shown that each subdetector meets all the mechanical and functional requirements. The engineering model of PAMELA is under construction. The integration on board of the Resurs satellite will start in 2001. The launch is foreseen for late 2002/early 2003.

References

[1] A. Bakaldin et al., Astro part physics 8 (1997) 109.
[2] V. Bidoli et al., Astrophys. J. Suppl. (to be published), Astro-ph/0012286.
[3] M. Ambriola et al., CAPRICE98: a balloon-borne magnetic spectrometer equipped with a gas RICH and a silicon calorimeter to study cosmic rays, Nucl. Instr. and Meth. A 461 (2001) 269, these proceedings. See also the references therein.
[4] O. Adriani et al., Nucl. Instr. and Meth. A 409 (1998) 447.
[5] O. Adriani et al., 3rd International Conference on Large Scale Appl. and Rad. Hard. of Semic. Det., Firenze, 1999, Il Nuovo Cimento, to appear.
[6] R. Turchetta, Nucl. Instr. and Meth. A 335 (1993) 44.
[7] J.H. Admas, et al., Proceedings of 26th ICRC, Salt Lake City, 1999, The CR-1 chip: Custom VLSI Circuitry for Cosmic Rays, OG.4.1.18.
[8] E. Barbarito et al., Nucl. Instr. Meth. A 313 (1992) 295.
[9] R. Bellotti et al., Nucl. Phys. B 54 (1997) 375.